ELSEVIER

Ceramics International 26 (2000) 363–370

CERAMICS INTERNATIONAL

Surface modification of ceramics for improved tribological properties

K.-H. Zum Gahr*, J. Schneider

University of Karlsruhe, Institute of Materials Science II and Forschungszentrum Karlsruhe, Institute of Materials Research I, PO Box 3640, 76021 Karlsruhe, Germany

Received 12 July 1999; received in revised form 29 July 1999; accepted 29 July 1999

Abstract

Surface modification of commercially available alumina ceramic was carried out by using laser irradiation for remelting and alloying. It is shown that resulting multiphase structures in the 100–400 μm thick surface zone can effectively reduce friction and wear in unlubricated oscillating sliding contact against Al_2O_3 counterbodies. Effect of microstructural parameters and experimental conditions such as counterbody, humidity and temperature are discussed. Transition behaviour from mild to severe wear is explained on the basis of a theoretical model.

Keywords: D. Alumina (Al_2O_3); Surface modification; Tribology; Multiphase ceramic

1. Introduction

Advanced alumina ceramics offer a high potential for structural components due to low density, high hardness, stiffness, temperature stability and corrosion resistance. Among other things, alumina is used for tribological applications such as seal rings, draw-cones, guides, bearing parts, cutting tools or medical prostheses. However, monolithic alumina can suffer severe problems under very high tribological and/or mechanical loads owing to its inherent brittleness and lack of defect tolerance, which can result in low wear resistance and a relatively high friction coefficient in self-mated unlubricated sliding contact [1,2].

As a function of operating conditions (e.g. load, speed, temperature, humidity) a transition from mild to severe wear occurs during sliding contact of self-mated alumina [2–4]. Mild wear can be characterized by a relatively low friction coefficient and a wear coefficient [1] $k < 10^{-6}$ mm^3 N^{-1} m^{-1} (k = wear volume divided by load and sliding distance). It is mainly determined by tribochemical reaction layers, plastic deformation, microabrasion and localized pull-outs of single grains. On the other hand, severe wear is connected with a high friction coefficient and wear coefficient owing to cracking under high tensile stresses at the rear end of the tribological contact, microfracture with grain pull-outs and formation of thick interfacial layers consisting of densified wear debris.

All tribologically induced interactions between two solids mated in sliding contact are concentrated on a relatively thin surface zone. Hence, it may be sufficient and economical to modify the microstructure for improved tribological performance in a surface zone of a thickness of a few hundred micrometers only. For this reason, surface modification was carried out on a commercial Al_2O_3 ceramic by remelting and alloying.

2. Materials and experimental methods

Surface treatment using a CO_2 laser was carried out on a commercially available Al_2O_3 ceramic (Al24, Fa. Friatec) with less than 5 vol% open porosity. Fig. 1 shows schematically the two different processes used for surface modification. In the first process (Fig. 1a), the as-delivered ceramic was coated by a suspension consisting of hafnia (HfO_2) or titanium nitride (TiN) powder, respectively, mixed with isopropyl alcohol. After drying of this precoating, the specimens were heated up to 1200–1500°C and then laser treated using an average

* Corresponding author. Tel.: +49-7247-823897; fax: +49-7247-824567.
E-mail address: zumgahr@imf.fzk.de (K.-H. Zum Gahr).

0272-8842/00/$20.00
PII: S0272-8842(99)00065-6

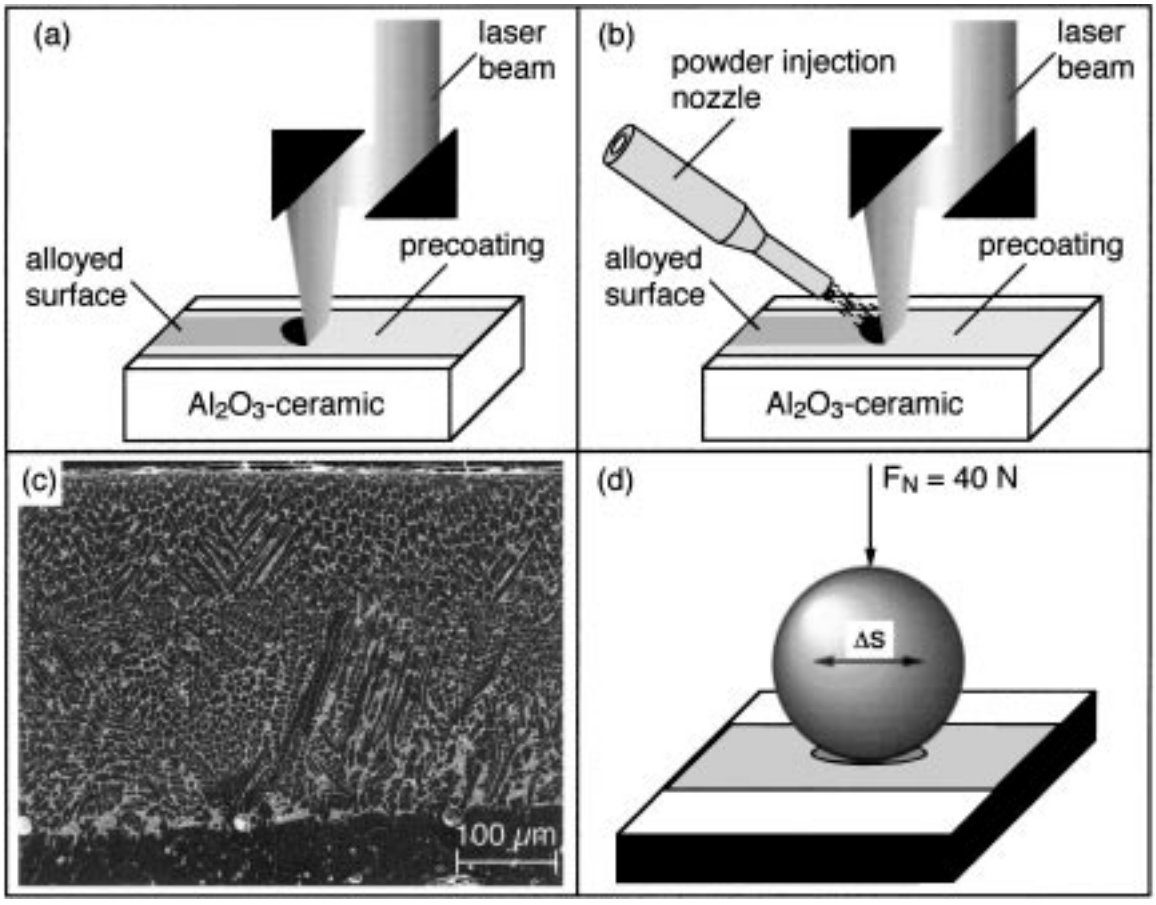

Fig. 1. Experimental set-up for laser treatment with (a) precoating process and (b) injection process. (c) Scanning electron micrograph of a cross-section through the surface modified ceramic A124Hf perpendicular to the travel direction of the laser beam and (d) tribological system (ball-on-block) used in oscillating sliding wear tests.

power range of about 200 W. Additional information is given elsewhere [5]. In the second process (Fig. 1b), the as-delivered ceramic was precoated by a zirconia (ZrO_2) powder and then heated up to 1500°C in laboratory air. At this temperature, the precoated surface was melted using the infrared laser irradiation with a beam integrator, which generated a rectangular beam cross-section of 1×6 mm^2 resulting in surface strips of 6 mm width. A commercial powder feeder was used to convey tungsten (W) powder to the injection nozzle and finally into the melt bath [6]. During laser treatment and following cooling to room temperature the specimens were protected by an argon gas shield for preventing oxidation. Chemical composition and properties of the different ceramics and the tribological counterbodies are presented in Table 1. Microstructure of the ceramics and worn surfaces were analyzed using standard ceramographic techniques, scanning electron microscopy (SEM) and energy dispersive X-ray spectroscopy (EDX).

Tribological properties were measured, using a laboratory tribometer (ball-on-block geometry, Fig. 1d) under unlubricated oscillating sliding contact against balls of 10 mm diameter of Al_2O_3, cemented carbides WC6Co and bearing steel 100Cr6 (1% C, 1.5% Cr), respectively. Before testing, all ceramic block specimens were ground by using different diamond discs, which resulted in an average surface roughness of R_a (c.l.a.) $\leqslant$ 0.1 µm. The grinding procedure led to a removal of a surface layer, of a thickness between 60 and 100 µm. The balls used as counterbodies showed an average surface roughness of $R_a = 0.08$ µm for Al_2O_3, and of $R_a = 0.09$ µm for both WC6Co and 100Cr6. The tests were run at a constant normal load of 40 N, a frequency of oscillation of 20 Hz and a stroke of 0.5 mm, which resulted in an average sliding speed of 0.02 m/s. The number of 1.44×10^5 oscillation cycles led to a total wear path length of 0.144 km. All tribological tests were carried out inside a climate chamber in which the relative humidity (RH) or the temperature were varied systematically. During each test, friction force and amount of total linear wear W_l (sum of ball and block wear) were measured continuously. After the tests, linear wear W_l* of the balls and the blocks was determined separately from surface profiles recorded by a stylus profilometer. All tribological results presented are average values of at least two individual tests.

3. Results

3.1. Microstructure

Fig. 1c shows a scanning electron micrograph of a cross-section through the laser-alloyed ceramic Al24Hf. Thickness of the alloyed surface layers could be varied between about 100 and 400 μm depending on the process parameters and the chemical composition used. Microstructures of the alloyed ceramics Al24TiN, Al24Hf and Al24WZ as well as the commercially available monolithic ceramic Al23 used for reference are presented in Fig. 2. The dense ceramic Al23 exhibited an average grain size of 6.5 μm and hardness of 2030 HV_{500} (Fig. 2a, Table 1). The ceramic Al24 used as substrate material for laser alloying contained an open porosity of less than 5 vol% and an average grain size of 30 μm with a bimodal size distribution range from 5–10 μm to 50–100 μm, respectively. Laser remelting of Al24 precoated with TiN particles of size between 1 and 5 μm resulted

Table 1
Materials, additives and microstructural parameters of the as-delivered ceramics (Al23, Al24), the laser surface-modified ceramics (Al24TiN, Al24Hf, Al24WZ) and the balls (Al_2O_3, 100Cr6, WC6Co) used as counterbodies in the tribological tests

Materials designation	Blocks					Balls		
	Al24	Al24TiN	Al24Hf	Al24WZ	Al23	Al_2O_3	100Cr6	WC6Co
Added compounds	–	TiN	HfO_2	$W + ZrO_2$	–	–	–	–
Average powder size (μm)	–	1.5	1.5	W: 6.8 ZrO_2: 1.3	–	–	–	–
Al_2O_3 matrix (vol%)	100	72	75	45	100	100	–	–
Grain boundary phase (vol%)	–	16	25	35	–	–	–	–
Reinforcing particles (vol%)	–	TiN:12	–	W:20	–	–	–	WC94
Average grain size (μm)	30	4	11	10	6.5	9	6	WC: 1-2
Hardness (HV_{500})	1900	1900	1750	1250	2030	1700	975	1700
Fracture toughness ($MPam^{1/2}$)	< 3	4.5	4.6	5.0	3.7	3–4	19	8.5

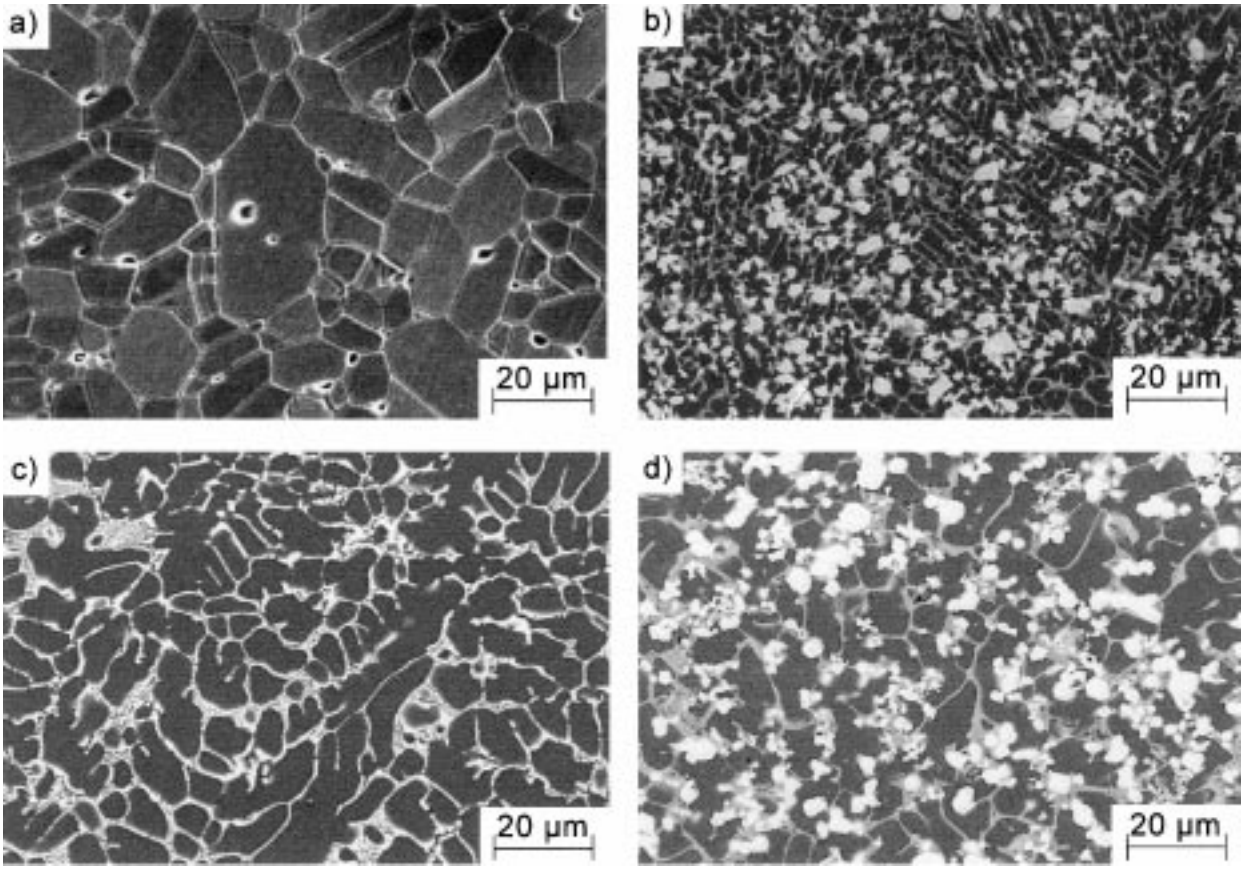

Fig. 2. Scanning electron micrographs of the (a) monolithic alumina ceramic A123 and surface-modified ceramics (b) A124TiN, (c) A124Hf and (d) A124WZ.

in a multiphase microstructure (Fig. 2b) consisting of 12 vol% TiN, 16 vol% of a Ti–O–Al grain boundary phase and balance alumina. Average size of the columnar Al_2O_3 crystallites was about 4 μm (Table 1). Alloying with hafnia powder led to fine lamellar eutectic phases along the Al_2O_3 boundaries in the ceramic Al24Hf (Fig. 2c) whereby volume fraction of this soft phase was about 25%. Laser remelting of ZrO_2 precoated alumina and injection of tungsten particles resulted in a microstructure Al24WZ containing Al_2O_3 crystallites of about 10 μm average size. Tungsten particles of an average size of 7 μm and of a volume fraction between 18 and 22% were distributed homogeneously in the grain boundary phase (about 35 vol%) and Al_2O_3 crystallites (Fig. 2d). According to Table 1, hardness of the alloyed surface structures decreased in the order of Al24TiN, Al24Hf and Al24WZ. Simultaneously, the indentation fracture toughness K_{Ic}* increased from about 4.5 $MPam^{1/2}$ (Al24TiN) up to about 5 $MPam^{1/2}$ (Al24WZ) which was substantially greater than that of the commercial ceramics Al24 and Al23, respectively.

3.2. Tribological properties

The effect of counterbody, relative humidity and temperature on friction and wear was systematically studied in the tribological tests.

Fig. 3 shows friction coefficient and amount of linear wear for the different ceramics mated with Al_2O_3 balls as a function of length of wear path in laboratory air at 50% RH and 28°C. After a short running-in period, the friction coefficient increased on the self-mated alumina pair (Al_2O_3/Al23) sharply to a maximum value of almost 1 before it went over with prolonged time to a quasi-stationary value of about 0.7 (Fig. 3a). Lowest values of friction coefficient were measured on the pair Al_2O_3/Al24WZ. The pairs Al_2O_3/Al24Hf and Al_2O_3/Al24TiN showed a slightly higher coefficient of friction but a very smooth course without irregularities with prolonged running-time, Al_2O_3/Al24TiN particularly. Wear of the self-mated pair with Al23 increased strongly during the running-in period owing to substantial wear of the Al_2O_3 ball. Compared with this alumina pair, amount of wear of the pairs with multiphase ceramics was up to the factor of about 9 lower after a wear path length of 144 m. The running-in period of these ceramics was substantially less marked. After 144 m length of wear path, the lowest amount of wear was measured on the pairs Al_2O_3/Al24TiN and Al_2O_3/Al24Hf.

Fig. 4 shows SEM micrographs of the ceramics Al23, Al24TiN, Al24Hf and Al24WZ after wear owing to unlubricated sliding contact against Al_2O_3 balls at room temperature and 50% RH. Self-mating of alumina (Fig. 4a) resulted in partially cracked interfacial layers consisting of densified wear debris and loose wear particles in the area of contact. In contrast, the surface modified structures Al24TiN, Al24Hf and Al24WZ (Fig. 4b–c) displayed smooth or rather polished surfaces after 144 m of oscillating sliding contact. Particularly, the worn surface of Al24TiN (Fig. 4b) was covered with small rolls owing to detached films produced by tribochemical reaction. Surfaces of the ceramic Al24WZ (Fig. 4d) exhibited locally deep grooving owing to abrasion which can be attributed to the lowest hardness value of all ceramics tested.

Fig. 5 shows the effect of the type of counterbody used, i.e. Al_2O_3, 100Cr6 or WC6Co ball, on friction and wear of the different sliding pairs. Lowest values of friction coefficient (Fig. 5a, μ about 0.35) were measured in mating balls of cemented carbides WC6Co against Al24Hf and Al24WZ, respectively. Highest values occurred if the ceramics were mated with steel balls 100Cr6. Fluctuations between highest and lowest values ($\mu_{max}-\mu_{min}$) measured during the quasi-stationary period of the tribotest was smallest in the pairs with WC6Co balls.

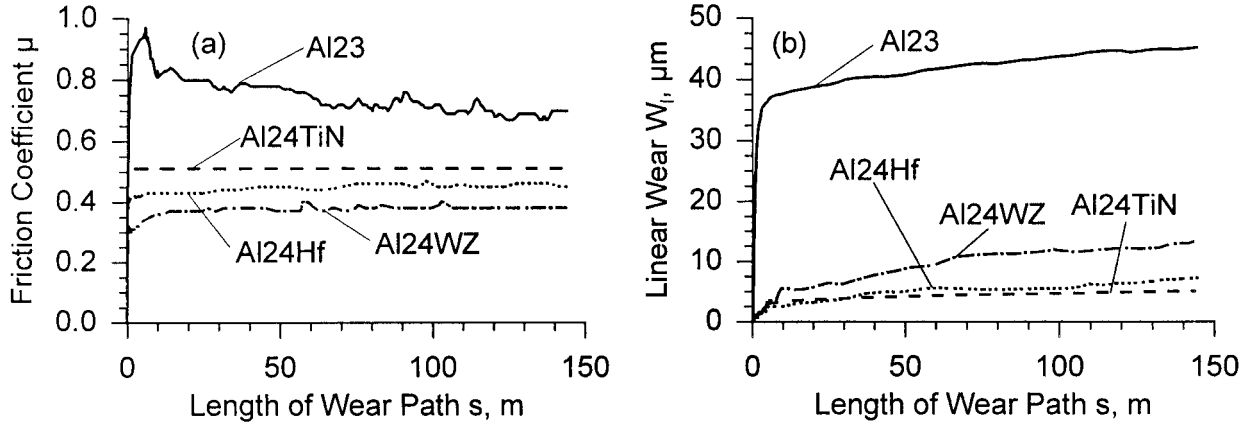

Fig. 3. (a) Friction coefficient μ and (b) amount of linear wear W_1 of the different ceramics under oscillating sliding contact against Al_2O_3 balls (at 28°C, 50% RH) versus length of wear path.

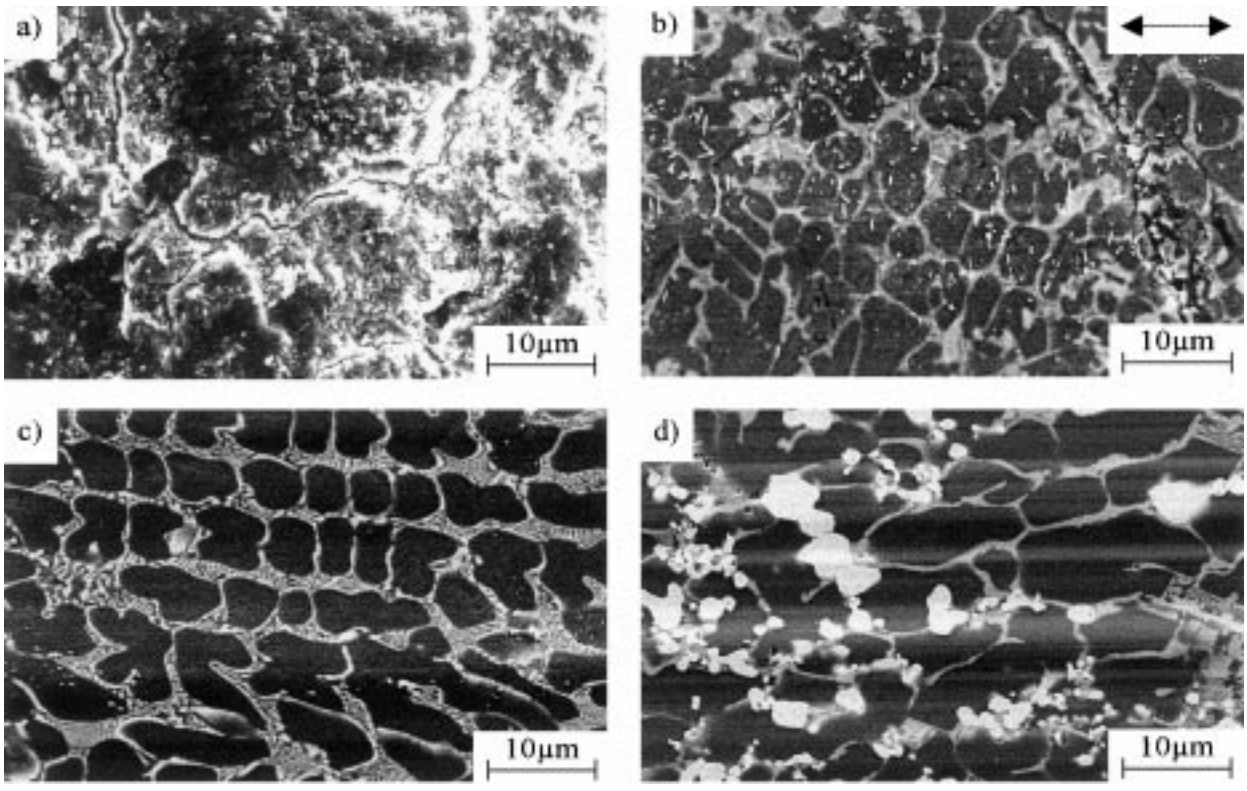

Fig. 4. SEM micrographs of surfaces of (a) A123, (b) A124TiN, (c) A124Hf and (d) A124WZ worn during oscillating sliding contact against Al_2O_3 balls (at 28°C, 50% RH) over a sliding distance of 144 m.

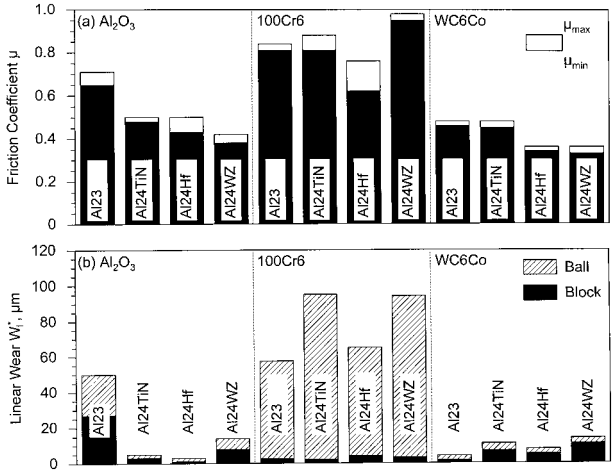

Fig. 5. (a) Friction coefficient and (b) amount of linear wear W_1* of the different ceramics in oscillating sliding contact (at 28°C, 50% RH) against Al_2O_3, 100Cr6 and WC6Co balls, respectively.

Amounts of linear wear as a function of type of counterbody (Fig. 5b), measured by using profilometry after 144 m length of wear path, did not exhibit a strong correlation with values of friction coefficient. Despite relatively high values of friction coefficient, the Al_2O_3 balls mated with Al24Hf and Al24TiN resulted in a very low amount of wear, comparable with that of WC6Co balls in sliding contact with alumina Al23. It is obvious from Fig. 5b, that the high amount of wear in the pairs with steel 100Cr6 was caused by severe damage of the balls. Material transfer from the steel balls to the ceramic block specimens led to sliding contact between steel/steel and/or iron oxide/iron oxide, respectively, and resulted in both high wear and friction coefficients.

Fig. 6 shows the effect of humidity or distilled water as interfacial medium on friction and wear of the ceramics during sliding contact against Al_2O_3 balls. Independently of the sliding pairs, the highest values of friction coefficient and linear wear were measured in dry air of 3% relative humidity and the lowest values if distilled water was present in the contact area. It becomes obvious that the tribological properties of both friction and wear of the pairs with Al24TiN depended strongly on humidity. Increasing the relative humidity from 3 to 35% resulted in a drop of amount of wear by a factor greater than 20 and friction coefficient by a factor of 2 after 144 m length of wear path (Fig. 6c and d). Above 35% RH, friction and wear of the Al24TiN pair were almost independent of humidity. Lower amount of wear on the pair Al_2O_3/Al23 with increasing humidity was caused by reduction of the ball wear by the factor of 3 primarily.

Fig. 7 shows friction coefficient and amount of wear of the self-mated alumina and the Al_2O_3/Al24TiN pair

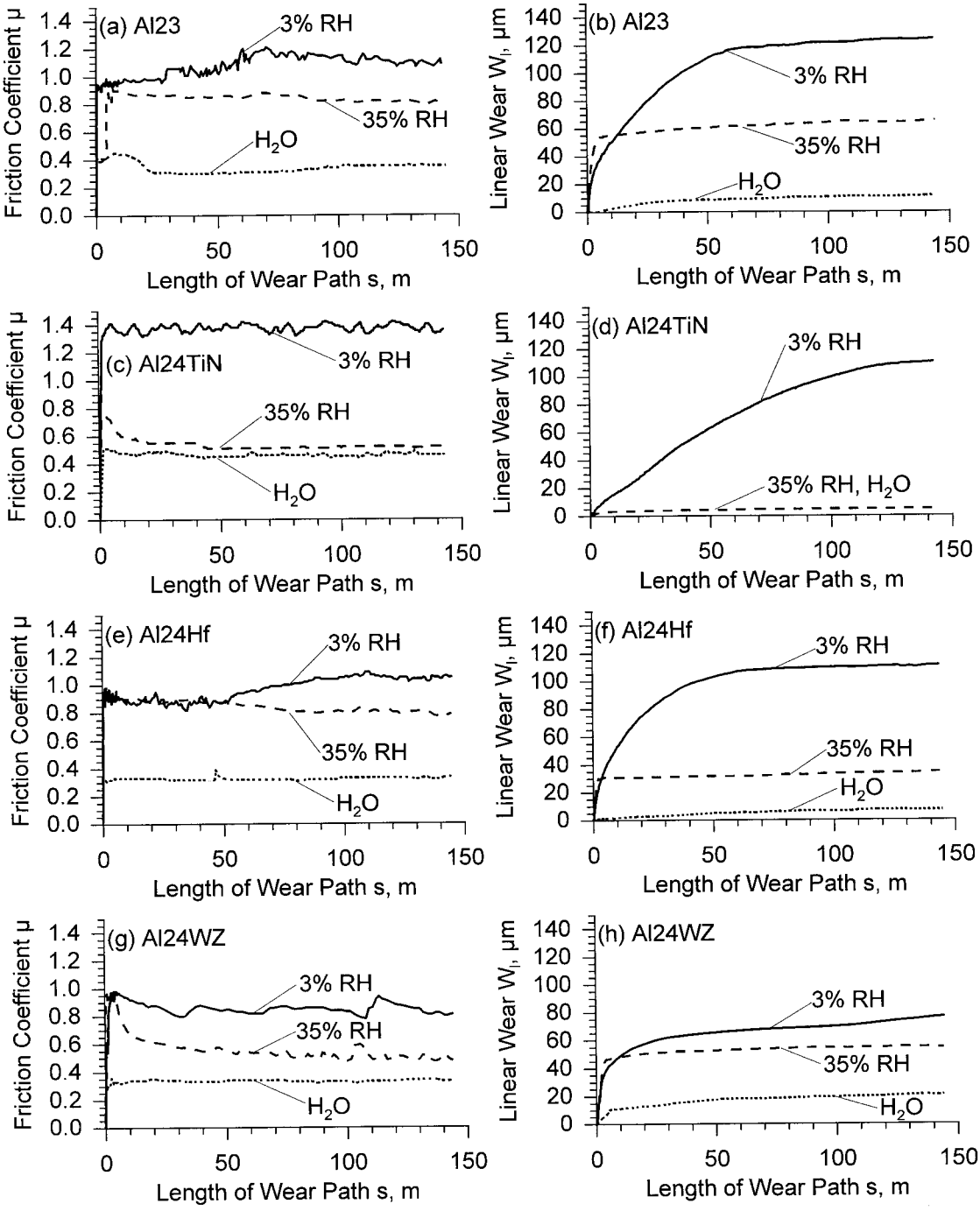

Fig. 6. Friction coefficient and amount of linear wear W_1 of the ceramics (a,b) A123, (c,d) A124TiN, (e,f) A124Hf and (g,h) A124WZ at relative humidities (RH) of 3 and 35% as well as with distilled water versus length of wear path against Al_2O_3 balls.

as a function of test temperature in air. Increasing test temperature from 28 to 110°C led to an increase of the quasi-stationary friction coefficient for the sliding pair Al_2O_3/Al23 from average values of about $\mu = 0.75$ to 1.05 (Fig. 7a). Simultaneously amount of wear of the pair (Fig. 7b) increased and particularly that of the block specimen. Both friction coefficient and amount of wear were nearly independent of test temperature between 110 and 500°C. For the pair Al_2O_3/Al24TiN (Fig. 7c), friction coefficient increased from the average value of 0.5 at 28°C to 1 at 250°C followed by decreasing values with further increasing test temperature up to 500°C. About equal values of friction coefficient were measured at 28 and 500°C. In agreement with the course of friction coefficient, the greatest amount of wear occurred at a test temperature of 250°C (Fig. 7d). At all temperatures, block wear was substantially greater than wear of the Al_2O_3 balls.

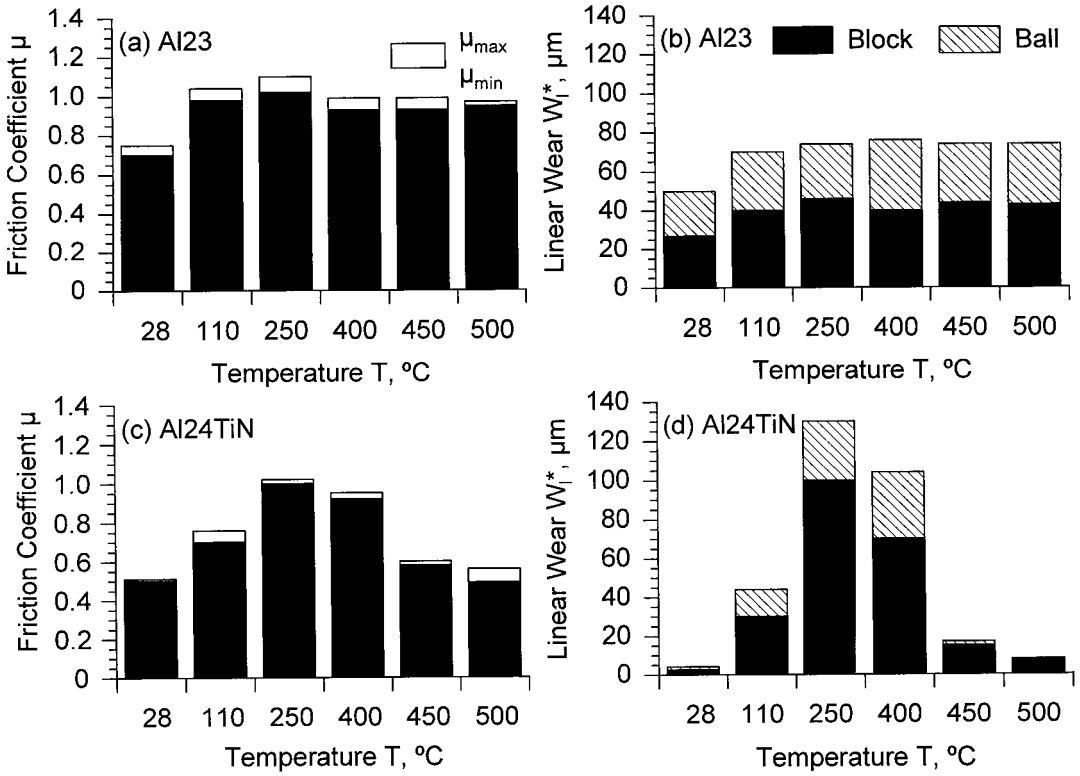

Fig. 7. Friction coefficient μ and amount of linear wear W_1* of (a,b) A123 and (c,d) A124TiN in oscillating sliding contact against Al_2O_3 balls as a function of test temperature.

4. Discussion

The experimental results show that surface modification of commercially available alumina ceramic by using laser remelting and alloying can be very effective for reducing friction and wear in unlubricated sliding contact. According to theoretical modeling [7] for ball-on-block geometry, friction coefficient depends on the type of interaction between the mated surfaces, e.g. elastic, plastic ploughing, microfracture etc. To a very first assumption, friction coefficient should depend in a given system (normal load, sliding speed, ball radius, ratio of apparent to true area of contact etc. are constant) on

$$\mu \propto \frac{\tau_s}{H^{3/2}} \tag{1}$$

for ploughing contact. Transition from mild to severe wear as a result of microfracture above a critical contact pressure p_{crit} can formally be described by

$$p_{crit} \propto \frac{K_{Ic}^* \cdot H}{\mu \cdot D^{1/2} \cdot E^{1/2}} \tag{2}$$

where τ_s =shear resistance or strength between the contacting surfaces, H = hardness, E = Young's modulus, $D = Al_2O_3$ grain size, K_{Ic}* = indentation fracture toughness and μ = friction coefficient. Considering Eqs. (1) and (2) it may be concluded for the present study that multiphase ceramics consisting of hard (TiN) and/or soft (HfO_2, W) phases embedded in the Al_2O_3 matrix can be beneficial for improving tribological performance owing to following effects.

Friction coefficient [Eq. (1)] should be reduced by thin surface films (aluminium hydroxide on alumina and/or TiO_{2-x} on TiN with Al24TiN) of low shear resistance τ_s and small contact area owing to large hardness H. This is supported by decreasing friction coefficient with increasing humiditiy (Fig. 6) which favours formation of AlOH. Increasing test temperature with Al24TiN (Fig. 7c) reduced AlOH surface films and led to enhanced friction. At 400°C and above TiO_{2-x} films can be formed on the TiN particles or the Ti–O–Al grain boundary phase and reduce friction coefficient. A soft oxide phase such as hafnia (Al24Hf) or a metallic phase such as tungsten (Al24WZ) reduced friction coefficient at and above 50% relative humidity effectively, i.e. also at lower temperatures (< about 100°C) only. In the presence of a water film (Fig. 6), the monolithic ceramic (Al23) and/or multiphase ceramics (HfO_2 in Al24Hf, W and ZrO_2 in Al24WZ) led to slightly lower friction coefficient than the ceramic Al24TiN containing hard TiN particles which may reflect the different wetting behaviour.

Critical contact pressure for transition from mild to severe wear [Eq. (2)] should be increased by increasing

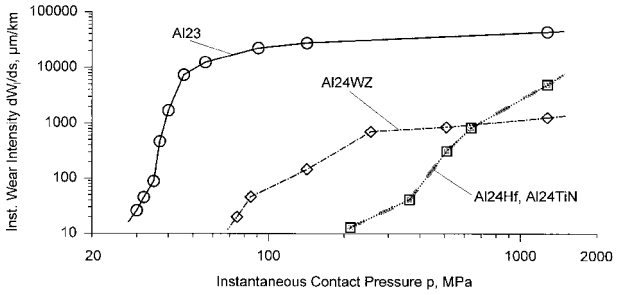

Fig. 8. Instantaneous wear intensity dW_1/ds of the different ceramics mated with Al_2O_3 balls (at 28°C, 50% RH) versus calculated instantaneous contact pressure p.

fracture toughness and avoiding of grain pull-outs. Hence, reinforcement by soft and/or hard particles, ductile grain boundary phases (high grain boundary fracture toughness [8]), small average grain size and/or elongated grain shape and low friction coefficient are beneficial for high values of p_{crit}. The ceramic Al24TiN (Table 1, Fig. 2) showed a very small average grain size, hard reinforcing TiN particles and a soft grain boundary phase which led to $K_{Ic}^{*} = (4.5 \pm 0.5)$ MPam$^{1/2}$ at hardness of 1900 HV_{500}. An equal value of K_{Ic}* was measured on Al24Hf at simultaneously lower hardness owing to 25 vol% of soft eutectic grain boundary phase which resulted in high grain boundary fracture toughness. Friction coefficient of Al24Hf was lower than that of Al24TiN mated with Al_2O_3 balls at 28°C and 50% RH (Fig. 3a). From the foregoing a similar transition behaviour in wear of both Al24TiN and Al24Hf may be expected. Fig. 8 shows a good qualitative agreement between the experimental transition from mild to severe wear intensity with increasing contact pressure and the simple model [Eq. (2)]. In this figure, the instantaneous wear intensity (slope of the curve W_1 versus length of wear path s) is plotted over the instantaneous contact pressure which was calculated from the ratio F_N divided by the apparent contact area $A(s)$, where $A(s) = \pi[2R - W_1(s)]W_1(s)$ and $2R$ is the diameter of the Al_2O_3 ball. At the beginning of the tests, a point contact prevails which changes into an area contact with increasing sliding length and wear, i.e. these tests were run from high to low apparent contact pressure [7]. It becomes obvious, that for both Al24TiN and Al24Hf the transition from mild to severe wear or reverse occurs at substantially greater p_{crit} values than for the other ceramics tested. Lower wear intensity of Al24WZ at high contact pressure (Fig. 8) compared with Al24TiN and Al24Hf can be explained by the about 15% lower Hertzian contact pressure at the beginning of the test owing to the low Young's modulus of 260 GPa for Al24WZ and 380–400 GPa for the other ceramics.

References

[1] H. Czichos, D. Klaffke, E. Santner, M. Woydt, Advances in tribology: the materials point of view, Wear 190 (1995) 155–161.
[2] K. Adachi, K. Kato, N. Chen, Wear map of ceramics, Wear 203–204 (1997) 291–301.
[3] S. Jahanmir, X. Dong, Wear mechanisms of aluminium oxide ceramics, in: S Jahanmir (Ed.), Friction and Wear of Ceramics, M. Dekker, New York, 1994, pp. 15–49.
[4] S.M. Hsu, V.S. Nagarajan, Haiyan Liu, Chuan He, Microstructural design of ceramics for wear, in: Proc. Int. Tribology Conference, Yokohama 1995, pp. 427–432.
[5] S.-Z. Lee, K.-H. Zum Gahr, Laser-induced surface alloying of Al_2O_3 ceramics with ZrO_2–TiO_2 powders, Ceram. Int. 20 (1994) 147–151.
[6] K. Przemeck, K.-H. Zum Gahr, Microstructure and tribological properties of alumina ceramic with laser-dispersed tungsten additions, J. Mater. Sci. 33 (1998) 4531–4541.
[7] K.-H. Zum Gahr, Modeling and microstructural modification of alumina ceramic for improved tribological properties, Wear 200 (1996) 215–224.
[8] A. Krell, D. Klaffke, Effect of grain size and humidity on fretting wear in fine-grained alumina, Al_2O_3/TiC, and Zirconia, J. Am. Ceram. Soc. 79 (1996) 1139–1146.